STUDY OF NATURAL GLASSES THROUGH THEIR BEHAVIOR AS MEMBRANE ELECTRODES, PART 2

by Alfred H. Truesdell, 1933-

U. S. Geological Survey

OPEN FILE REPORT

62-136

This report is preliminary and has not been edited or reviewed for conformity with Geological Survey standards or nomenclature.

Weld - Int. 2905

UNITED STATES
DEPARTMENT OF THE INTERIOR
GEOLOGICAL SURVEY
Washington, D. C.

For release JULY 23, 1962

The Geological Survey is releasing in open files the following reports. Copies are available for consultation in the Geological Survey Libraries, 1033 GSA Bldg., Washington, D. C.; Bldg. 25, Federal Center, Denver, Colo.; and 345 Middlefield Rd., Menlo Park, Calif.; plus other offices as listed:

1. Geology and coal resources of the Carbondale area, Garfield, Pitkin and Gunnison Counties, Colorado, by John R. Donnell. 1 map, 1 table. On file at 468 New Custom House, Denver, Colo.; and 437 Federal Bldg., Salt Lake City, Utah. Copies from which reproductions can be made at private expense are available in the Library, Bldg. 25, Federal Center, Denver, Colo.

2. Preliminary report on the stratigraphy of Paleozoic rocks southwest of Pocatello, Idaho, by D. E. Trimble and W. J. Carr. 16 p., 2 figs. On file at 437 Federal Bldg., Salt Lake City, Utah; South 157 Howard St., Spokane, Wash.; and in the office of the Idaho Bureau of Mines and Geology, Moscow, Idaho.

3. Geologic maps showing outcrops of the Nonesuch shale from Calumet to Black River, Michigan, by W. S. White and J. C. Wright. 2 maps. On file at 222 Science Hall, University of Wisconsin, Madison, Wis.; Office of the State Geologist, Dept. of Conservation, Lansing, Mich.; Library, Michigan College of Mining and Technology, Houghton, Mich.

4. TEI-814. Interim geological investigations in the U12b.08 tunnel, Nevada Test Site, Nye County, Nevada, by W. L. Emerick and F. N. Houser. 23 p., 3 figs., 5 tables. On file at 232 Appraisers Bldg., San Francisco, Calif.; 1031 Bartlett Bldg., Los Angeles, Calif.; 437 Federal Bldg., Salt Lake City, Utah; Library, Mackay School of Mines, University of Nevada, Reno, Nev.; 279 Geology Bldg., University of New Mexico, Albuquerque, N. Mex.; USGS office, Mercury, Nev.

5. TEI-816. Thermodynamic properties of minerals, by Richard A. Robie. 31 p., 1 table.

The following report is also released in open files, but is available only at the Geological Survey library, 1033 GSA Bldg., Washington, D. C.:

6. Study of natural glasses through their behavior as membrane electrodes, Part 2, by Alfred H. Truesdell. 43 p., 14 figs., 2 tables.

Contents

Study of Natural Glasses Through Their Behavior as Membrane Electrodes, Part 2

By Alfred H. Truesdell

Abstract

The exchange constants and regular solution constants for a number of exchange reactions involving analyzed natural and simulated natural glasses have been determined. The experimental method used provides quick and simple determination of these constants. The calculation of the internal energy differences of model ion exchange systems involving alkali and alkaline earth cations yields sequences (but not magnitudes) of selectivity that agree with the experimental results. Complex glasses such as obsidians, tektites and basaltic glasses do not in general show simple correlations between composition and ion exchange behavior.

Study of Natural Glasses Through Their Behavior as Membrane Electrodes, Part 2

Alfred H. Truesdell

Introduction

In studying the ion exchange reactions of rhyolitic natural glasses, it was discovered that they showed moderately large selectivity for alkaline earth cations (Truesdell, 1962). Although selectivity of glasses for alkali cations has been thoroughly explored experimentally and theoretically by Eisenman, Rudin and Casby (1957), and by Eisenman (1961), essentially nothing is known about the origin of selectivity for divalent cations. Accordingly, the ion exchange constants of a group of natural glasses with relatively large contents of alkaline earth oxides and with a wide compositional range were determined and calculations were made for idealized models of ion exchangers of the selectivities for alkali and alkaline earth cations.

I wish to thank Professor R. M. Garrels of Harvard University and Dr. C. L. Christ of the U. S. Geological Survey for the guidance, encouragement and friendly criticism that they have so freely given. I would like to thank my colleagues at the U. S. Geological Survey, Dr. E. C. T. Chao for specimens of analyzed tectites, Frank Reed for many skillfully prepared thin sections, and H. J. Rose, Jr., F. J. Flanagan, and L. Shapiro for rock analyses by X-ray fluorescence and rapid chemical methods. I would also like to thank Dr. M. Nordberg and Dr. W. H. Dunbaugh of Corning Glass Works for the preparation of the synthetic glasses.

Experimental

Ion exchange constants of ten natural and simulated natural glasses (analyses in Table 1) were determined by the experimental method described earlier (Truesdell, 1962). The glass to be studied was ground to a thin membrane and cemented to an ordinary glass tube. This tube was filled with 0.01 m HCl and a silver wire was inserted. The completed membrane electrode was immersed together with a reference electrode having a saturated KCl liquid junction in a salt solution containing a known activity of one of the exchangeable cations. Increments of second salt were added and the equilibrium potential of the membrane electrode (as measured with a high impedance vibrating capacitor electrometer) and the activity of each cation were recorded after each increment. In most of the experiments, glass electrodes specifically sensitive to H^+, Na^+, and K^+ and insensitive to alkaline earth cations and anions were used to measure activities. In each case the electrode was calibrated with a standard solution of known activity of a given ion (s), and the activity of the ion in the test solution after each increment was calculated from the equation (using H^+ ion here as a specific example)

$$\log a_{H^+} + \log a_{H^+,s} + \frac{E - E_s}{2.303(RT/\mathcal{F})},$$

where E is the potential of the glass electrode relative to a calomel electrode in the test solution and E_s its potential relative to a calomel electrode in the standard solution, a_{H^+} is the hydrogen ion activity in the test solution and $a_{H^+,s}$ is that of the standard

solution.

A pH electrode was used for the H^+-K^+ and H^+-Na^+ exchanges, a Na^+ specific electrode for Na^+-K^+ exchanges and a Na^+-K^+ electrode for the K^+-Ca^{++}, Na^+-Ca^{++} and Na^+-Mg^{++} exchanges. Except in the H^+-K^+ and H^+-Na^+ exchanges, a trace of $Ca(OH)_2$ was used to suppress the a_{H^+} to at least five orders of magnitude below that of the other cations. A saturated KCl-calomel electrode was used as a reference and the connection to the test solution was made through an asbestos fiber wick to minimize KCl contamination. In some cases the measured potential was somewhat instable; this was corrected by cleaning the wick.

For each exchange the potential of the test electrode was plotted against the log of the activity of the cation added. These points were fitted to an electrode curve by comparison with a family of calculated curves (figure 1).

Each curve in figure 1 was obtained by assuming a B_{AB} value and for various mole fractions on the glass calculating the activity of B^+ in solution for an assumed initial activity of A^+ from the exchange equation (assuming $K_{AB} = 1$).

$$\frac{\exp\left(\frac{B_{AB}}{RT} N_{BX}^2\right) N_{AX}[B^+]}{\exp\left(\frac{B_{AB}}{RT} N_{AX}^2\right) N_{BX}[A^+]} = 1$$

and finally calculating the electrode potential (assuming $E^o = 0$) by substituting the activities in solution and the activity coefficients in the glass into the electrode equation (Garrels and others, 1962).

$$E = E^{o} + \frac{RT}{2\mathcal{F}} \ln\left(\sum_{J=A}^{B} K_{AJ} \frac{[J^{2+}]^{2/z}}{\lambda_{J_{2/z}} X_2} \right)$$

where $\lambda_{J_{2/z}X_2} = \exp\left(\frac{B_{AB}}{RT} 1 - N_{J_{2/z}X_2} \right)^{2}$.

Two electrode curves for the K^{+}-Mg^{++} and K^{+}-Ca^{++} exchanges on a tectite from the Philippines (NG 6) are shown in figures 2a and 2b. The data for the second of these (figure 2b) was given in Table 3 of Garrels and others (1962).

In figure 2a, the first point recorded was the potential of the electrode in 200 ml of a 0.001 m KCl solution without any Mg^{++} added. About 0.01% $MgCl_2$ is present, however, as an impurity in the reagent grade KCl used so the activity of Mg^{++} in the solution is near 10^{-7}. Two successive 1.0 milliliter additions each of 0.001 m, 0.01 m and 0.1 m $MgCl_2$ were made and after each addition the equilibrium potential of the test electrode was recorded. The two straight lines (a, b) on the graph represent the potential the electrode would assume if the solution contained only Mg^{++} (a) or only 0.001 m K^{+} (b). The intersection of these lines is the activity of Mg^{++} alone that would produce the same potential as 0.001 m K^{+}. The electrode equation

$$E = E^{o} + \frac{2.303\,RT}{2} \log\left(\frac{[K^{+}]}{\lambda_{K_2X_2}} + K_{KMg} \frac{[Mg^{++}]}{\lambda_{MgX_2}} \right)$$

can be written when $[K^{+}] = 0$ and therefore $\lambda_{K_2X_2} = 0$ and $\lambda_{MgX_2} = 1$:

$$E_1 = E^{o} + \frac{2.303\,RT}{2} \log\left(K_{KMg} [Mg^{++}] \right)$$

and when $[Mg^{++}] = 0$ ($\lambda_{MgX_2} = 0$; $\lambda_{K_2X_2} = 1$)

$$E_2 = E^\circ + \frac{2.303\,RT}{2\mathcal{F}} \log [K^+]^2.$$

When activities of the cations are those that produce the same potential ($E_1 = E_2$)

$$\log (K_{KMg}[Mg^{++}]) = \log [K^+]^2$$

$$\log K_{KMg} = 2 \log [K^+] - \log [Mg^{++}].$$

In figure 2a $\log [K^+] = -3.016$, at the intersection $\log [Mg^{++}] = -4.21$. Therefore $\log K_{KMg} = -6.03 + 4.21 = -1.82$ and $K_{KMg} = 1.51 \times 10^{-2}$.

B_{AB} values are obtained directly from comparison with figure 1. E°, which depends largely upon the concentration of the solution inside the electrode, is determined from the difference between the observed potential E and the value of $(2.303\,RT/2\mathcal{F}) \log [K^+]^2$ before any Mg^{++} is added.

The curves calculated from the electrode equation fit the experimental results within the experimental error which indicates that the adsorbed ions form a symmetrical regular solution.

The constants B_{AB} and K_{AB} for each exchange are given in Table 2. The nomenclature is that used earlier (Truesdell, 1962).

During the experiments unusually large drifting of the asymmetry potentials between the two surfaces of the electrode membrane was noted. This has not been observed in alkali aluminosilicate glasses, (Eisenman, Rudin, and Casby, 1957), potassium barium aluminosilicate glasses or natural glasses with a low iron content (Garrels, et al., 1962). It is probable that in glasses with a high FeO content oxidation of ferrous iron in the surface exchangeable phase changes the

local charge density and alters the properties of the surrounding exchange sites. The external surface of the membrane having been exposed to large changes in pH and salinity would be expected to oxidize at a different rate from the inner surface of the membrane which is in contact with a dilute solution at a fixed pH and salt content. This produces drifting of the asymmetry potential.

Theoretical

The ion exchange constant K_{AB} is related to the standard free energy change, ΔF°_{r},[*] of the reaction:

$$AX_{glass} + B^{+}_{aq} = BX_{glass} + A^{+}_{aq}$$

by the equation $\Delta F^{\circ}_{r} = -2.303\ RT \log K_{AB}$.

ΔF°_{r} equals the sum of the standard free energies of formation, ΔF°_{f}, of the products, less that of the reactants:

$$\Delta F^{\circ}_{r} = \Delta F^{\circ}_{f,BX} + \Delta F^{\circ}_{f,A^{+}} - \Delta F^{\circ}_{f,AX} - \Delta F^{\circ}_{f,B^{+}}$$

The ΔF°_{f} of the alkali and alkaline earth cations have been determined experimentally and are tabulated in Rossini, Wagman, Evans, Levine and Jaffe (1952). The standard free energies of formation of the adsorbed ions cannot, however, be easily calculated.

The internal energy, ΔU, which is related at constant temperature and pressure to the free energy by $\Delta F = \Delta U + P\Delta V - T\Delta S$ can be calculated for simple models of the ion exchange process in which the ions

---

[*] Extensive thermodynamic quantities are molal throughout.

and the negative sites behave as rigid charged spheres with only electrostatic forces between them.*/

This model has been used by Eisenman (1961) to calculate the sequences of selectivity among the alkali cations and yielded an excellent qualitative correspondence with experimentally determined sequences.†/

Eisenman (1961a) calculated both ΔU_T^o and ΔF_T^o for exchanges involving the alkali cations and found that both quantities yielded

---

*/ To the extent that the internal energy is equivalent to the free energy in this system we can also write $\Delta U_T^o \simeq -2.303\ RT \log K_{AB}$.

†/ An alternate test of this model is the correspondence between calculated and experimental lattice energies of alkali and alkaline earth halides (Waddington, 1959). The differences are within ± 1% for the alkali halides and BeF_2, SrF_2, CaF_2 and MgF_2 and within ± 2% for $SrCl_2$. The agreement is less good for the alkaline earth bromides and iodides where the degree of polarization may be expected to be large. In the following analysis the effective anionic radius of the sites is equivalent to or smaller than that of the Cl^- ion so the energies calculated from an ionic model may be expected to be within ± 2% (or better) of the true values.

---

sequences of selectivity that correspond with experiment, and that the difference between ΔU_T° and ΔF_T° was, in general, small. Much larger differences in these quantities were found between anhydrous and hydrous systems.

The use of ΔU_T° as equivalent to ΔF_T° is justified for ion exchange systems because: (a) all phases are condensed so that $P\Delta V$ is small, (b) the absolute temperature is relatively low, and (c) the entropy differences between different ions in solution is small, and that between the ions adsorbed on the glass is very small, and thus, both $P\Delta V$ and $T\Delta S$ are small compared with the internal energy ΔU.

The exchange reaction can be divided into a set of reactions whose ΔU_T° can be separately calculated. These are:

$AX_{glass} = A^+_{gas} + X^-_{gas}$	ΔU_1°	$= \Delta U^\circ$ dissociation, AX
$B^+_{aq} = B^+_{gas}$	ΔU_2°	$= -\Delta U^\circ$ hydration, B^+
$A^+_{gas} = A^+_{aq}$	ΔU_3°	$= \Delta U^\circ$ hydration, A^+
$B^+_{gas} + X^-_{gas} = BX_{glass}$	ΔU_4°	$= -\Delta U^\circ$ dissociation, BX
$AX_{glass} + B^+_{aq} = BX_{glass} + A^+_{aq}$	ΔU_T°	$= \Delta U_1^\circ + \Delta U_2^\circ + \Delta U_3^\circ + \Delta U_4^\circ$.

The internal energy of dissociation, ΔU_1°, is equal to the electrostatic energy required to remove the ions to infinite separation from the distance of closest approach. ΔU_1° is given by the expression

$$\Delta U_1^\circ = + \frac{332}{r_A^+ + r_X^-},$$

where r_A^+ is the radius of the (monovalent) cation in closest possible packing, leading to minimum energy, with the (monovalent) anion of radius r_X^-, the radii being expressed in Angstroms; ΔU_1° is in Kcal

mole^{-1}.*/ Similarly $\Delta U_4^\circ = -\frac{332}{r_B^+ + r_X^-}$.

$\Delta U_2^\circ + \Delta U_3^\circ$ can be obtained from the experimentally determined standard enthalpies of formation (25°C) of the ions as a perfect gas and in aqueous solution.

$$\Delta U_2^\circ = \Delta H^\circ_{gas,B^+} - \Delta H^\circ_{aq,B^+} - P(V_{gas,B^+} - V_{aq,B^+})$$

$$\Delta U_3^\circ = \Delta H^\circ_{aq,A^+} - \Delta H^\circ_{gas,A^+} - P(V_{aq,A^+} - V_{gas,A^+}),$$

V_{gas,B^+} is very nearly equal to V_{gas,A^+} and V_{aq,B^+} is nearly equal to V_{aq,A^+}†/ so we can set:

$$\Delta U^\circ_{hyd,A^+} - \Delta U^\circ_{hyd,B^+} = \Delta H^\circ_{gas,B^+} + \Delta H^\circ_{aq,A^+} - \Delta H^\circ_{aq,B^+} - \Delta H^\circ_{gas,A^+}.$$

The values of ΔH° are tabulated in Rossini and others (1952). The

---

*/ The electrostatic force, F, between two ions is $F = \frac{z_1 z_2 e^2}{x^2}$ where e is the charge on the electron; z_1, z_2 the valence of the ions and x is the separation between them. The work of moving two oppositely charged monovalent ions to infinite separation from the distance of closest approach $(r^+ + r^-)$ is the integral over the distance, $\Delta U = \int_{(r^+ + r^-)}^{\infty} F dx =$ $[Fx]_{(r^+ + r^-)}^{\infty} = -\left[\frac{e^2}{x}\right]_{(r^+ + r^-)}^{\infty} = +\frac{e^2}{(r^+ + r^-)}$. The charge on the electron is 4.8021×10^{-10} statcoulombs so that since ergs = dyne cm = (statcoulombs)^2 cm^{-1}

$$\Delta U = \frac{(4.8021 \times 10^{-10})^2}{1 \times 10^{-8}} = 2.3061 \times 10^{-11} \text{ erg Angstroms molecule}^{-1}$$

To convert this to Kcal mole^{-1} Angstroms we must multiply by Avogadros number times Kcal erg^{-1}.

$$2.3060 \times 10^{-11} \times 6.0247 \times 10^{23} \times 2.390 \times 10^{-11} = 332.04$$

†/ The $P\Delta V$ difference between B^{++}_{gas} and $2A^+_{gas}$ is about one Kcal mole^{-1}. This has not been included in the calculations.

enthalpies of hydration (25°C), ΔH°_{hyd} (i.e., $\Delta H^{\circ}_{aq} - \Delta H^{\circ}_{gas}$), used in the calculations are (in Kcal mole^{-1}): Mg^{++}, -672.2; Ca^{++}, -593.4; Sr^{++}, -558.1; Ba^{++}, -524.4; $2Li^{+}$, -454.8; $2Na^{+}$, -406.6; $2K^{+}$ -366.2. Thus the internal energy change of the reaction

$$AX_{glass} + B^{+}_{aq} = BX_{glass} + A^{+}_{aq}$$

can be calculated as

$$\Delta U^{\circ}_{r} = - \frac{332}{r^{+}_{B} + r^{-}_{X}} + \frac{332}{r^{+}_{A} + r^{-}_{X}} + \Delta U^{\circ}_{hyd,A^{+}} - \Delta U^{\circ}_{hyd,B^{+}}$$

This is the basic equation for the calculations made by Eisenman (1961a).

Since the properties of water and the cation radii (r^{+})[*] are fixed, the variation in the exchange selectivity of various ion exchanges must depend solely on the effective radius of the exchange sites. In other words, the differences in the electronegativity of the oxygen ion in various silicate, alumino silicate and borosilicate glasses depend on the character of the adjacent electropositive ions and the local structure and can be represented by different values of the effective anionic radius. By varying r^{-}, Eisenman calculated 11 orders of selectivity among the five alkali cations and through a careful study of glasses in the system Na_2O-Al_2O_3-SiO_2 he was able to demonstrate that these 11, and only these 11, selectivity orders exist.

---

[*] The ionic radii used in the following calculations are: Li^{+}, 0.68 Å; Na^{+}, 0.98 Å; K^{+}, 1.33 Å; Mg^{++}, 0.66 Å; Ca^{++}, 0.99 Å; Sr^{++}, 1.16 Å; and Ba^{++}, 1.43 Å. These are taken from Green (1959) and Evans (1952).

In this paper these calculations have been extended to divalent cations; however, the experimental verification of the results is not complete.

In calculating the selectivities between the divalent cations there are more variations possible. The sites may be considered as either spherical divalent anions or as pairs of spherical monovalent anions at a variable separation, x. Each site may also, of course, have a variable effective anionic radius. Figure 3 shows the configurations for which the internal energy changes were calculated.

Divalent Sites

In figure 4 is shown the internal energy change, as a function of $r^{=}$, for the exchanges:

$$CaX + A^{++} = AX + Ca^{++},$$

and

$$CaX + 2B^{+} = B_2X + Ca^{++},$$

where $X^{=}$ is a divalent site of radius $r^{=}$, A^{++} is Mg^{++}, Ba^{++}, or Sr^{++}, and B^{+} is Li^{+}, Na^{+}, or K^{+}. The lower the internal energy, ΔU, of the reaction the greater the preference for that ion. Thus at an $r^{=}$ of 1.2 Å the order of decreasing preference is $2Li^{+} > 2Na^{+} > 2K^{+} > Mg^{++} > Ca^{++} > Sr^{++} > Ba^{++}$. The internal energy differences can be read from the graph and the equivalent K_{AB} computed from $\Delta U^{\circ}_{r} = -2.303\ RT \log K_{AB}$.

In computing the internal energy of interaction of a divalent cation with a divalent site the equation

$$\Delta U^{\circ} = -4\ \frac{332}{r^{++} + r^{=}}$$

was used. This corresponds to situation b in Fig. 3. For the interaction of monovalent ions with a divalent site the equation

$$\Delta U^{\circ} = -4 \frac{332}{r^{+} + r^{-}} + \frac{332}{2(r^{+} + r^{-})}$$

was used. This assumes that the monovalent cations arrange themselves on exactly opposite sides of the anion, according to the arrangement shown in Fig. 3c.

Paired Monovalent Sites with Separation, x.

If the exchange site is considered to be composed of two monovalent anions their separation is an important variable. Figure 5 shows the variation with site separation of the internal energy of the exchange

$$Na_2X_2 + Ca^{++} = CaX_2 + 2Na^{++}$$

for site radii, r^{-}, of 0.5 and 1.0 A.

Na^{+} is preferred over Ca^{++} at all but the smallest site separation. Thus, even on exchangers in which the exchange capacity is very high, monovalent ions are generally preferred.

To calculate the energy of interaction of the divalent cations with paired monovalent anionic sites at a separation of x Angstroms, the equation

$$\Delta U^{\circ} = -2 \frac{332}{r^{++} + r^{-}} -2 \frac{332}{x-(r^{++} + r^{-})} + \frac{332}{x}$$

has been used. This corresponds to the physical situation of Fig. 4e. For a pair of monovalent cations the equation

$$\Delta U^{\circ} = -2\frac{332}{r^{+} + r^{-}} - \frac{332}{x-(r^{+} + r^{-})} - \frac{332}{x + (r^{+} + r^{-})} + 2 \frac{332}{x}$$

corresponding to Fig. 3d.

Figures 6a and 6b show the selectivity relations among the alkali and alkaline earth cations on paired monovalent sites with separations of 12 Å and 4.5 Å.

Among the four alkaline earth cations there are seven orders of selectivity but the arrangement of the orders (and of the cations within the orders) depends on the site separation. This situation is quite different from that of the alkali cations where there is only a single set of 11 orders which is independent of site separation (Eisenman, 1961a).

The calculated orders of selectivity are for a large site separation (8 Å)

→ increasing anionic radius

↓ increasing preference

Ba	Ba	Ba	Ca	Ca	Mg
Sr	Ca	Ca	Ba	Mg	Ca
Ca	Sr	Mg	Mg	Ba	Ba
Mg	Mg	Sr	Sr	Sr	Sr

near 8 Å the order changes to

Ba	Ba	Ca	Ca	Ca	Mg	Mg
Sr	Ca	Ba	Ba	Mg	Ca	Ca
Ca	Sr	Sr	Mg	Ba	Ba	Sr
Mg	Mg	Mg	Sr	Sr	Sr	Ba

at 6 Å site separation the order is

Ba	Ba	Ca	Ca	Ca	Ca	Mg
Sr	Ca	Ba	Ba	Mg	Mg	Ca
Ca	Sr	Sr	Mg	Ba	Sr	Sr
Mg	Mg	Mg	Sr	Sr	Ba	Ba

Finally below 5 Å separation the order is

Ba	Ba	Ca	Ca	Ca	Ca	Mg
Sr	Ca	Ba	Sr	Sr	Mg	Ca
Ca	Sr	Sr	Ba	Mg	Sr	Sr
Mg	Mg	Mg	Mg	Ba	Ba	Ba.

Paired Monovalent Sites at the Minimum Separation about a Divalent Cation

The monovalent-divalent selectivity calculated assuming divalent sites (fig. 4) or pairs of monovalent sites with a fixed separation and variable effective anion radius (fig. 6) show a larger preference to monovalent ions than is observed in natural glasses, although the values are of the same order of magnitude observed by Eisenman and others (1957) for glasses in the system Na_2O-Al_2O_3-SiO_2. Probably the pertinent difference between these glasses and the natural glasses studied is the divalent metal oxides CaO, MgO, and FeO*/ in the natural glasses.

---

*/ Fe^{++} probably does not remain divalent in the hydrated surface phase of the glass where exchange takes place since the O_2 partial pressure should be near 0.2 atmospheres which is much greater than the equilibrium FeO - Fe_2O_3 pressure.

In order to test this a further calculation was made of the internal energy of the reactions

$$CaX_2 + 2A^+ = AX_2 + Ca^{++}$$

and

$$CaX_2 + B^{++} = BX_2 + Ca^{++}$$

with a variable effective anion radius and with the site separation varied so that the anions would be linearly arranged at the distance of closest approach to a Ca^{++} ion. The energy of interaction with the two monovalent sites was calculated from the equations

for Ca^{++}:

$$\Delta U = -4 \frac{332}{0.99 + r^-} + \frac{1}{2} \frac{332}{0.99 + r^-}$$

for Mg^{++}:

$$\Delta U = -2 \frac{332}{0.66 + r^-} - 2 \frac{332}{1.98 + r^- - 0.66} + \frac{1}{2} \frac{332}{0.99 + r^-}$$

for Na^+ or Li^+ */

$$\Delta U = -2 \frac{332}{r^+ + r^-} - \frac{332}{1.98 + 2r^- + (r^+ + r^-)}$$

$$- \frac{332}{1.98 + 2r^- - (r^+ + r^-)} + 2 \frac{332}{1.98 + 2r^-}$$

The resulting curves are given in Figure 7.

---

*/ A similar equation was used for K^+ with an additional factor in the positive term to allow for the K^+ ion between the sites being out of line since the distance between the sites is 1.98 Å and the diameter of a K^+ ion is 2.66 Å.

Discussion

The calculations of internal energy changes of ion exchange reactions show that alkali ions should be greatly preferred over alkaline earth ions on model ion exchangers consisting of either separate monovalent sites, divalent sites or paired monovalent sites at all but the smallest separations.

The magnitude of the calculated energy differences, as compared to observed values particularly between monovalent and divalent cations, is too great. Several factors may be involved, particularly the presence of water in the glass and variations in the actual arrangement of the monovalent cations on the negative sites. The presence of water in the glass sharply reduces the magnitude of ion exchange specificity but does not change the relative sequence of preference. This has been discussed by Eisenman (1961a). A second factor that would tend to reduce the large calculated preference for monovalent cations is the influence of alterations of the geometry of the cations on the negative exchange sites. The calculation of the internal energy of interaction of the monovalent cations with divalent negative sites (figure 4) or paired monovalent negative sites (figures 6 and 7) includes a positive term due to the repulsion of the two cations which could be much larger if the cations were not free to assume the maximum separation. The single divalent cation is not affected by such constraints. This steric factor could alter the magnitude and sequence of ion preference between monovalent and divalent ion groups. The sequence and magnitude of preference within each group will not be affected.

With these reservations about the calculated magnitudes of exchange energies, we can examine the model systems for their correspondence to natural glasses.

Anionic sites with two negative charges at a single point (figure 3b and c) cannot actually exist in these glasses since they are composed of oxygen polyionic frameworks in which at least half of the -2 charge of each oxygen ion is satisfied by Si^{+4} or Al^{+3}.

Paired monovalent negative sites (figure 3d, e and f) are more realistic and in general the correspondence between calculated and observed energy changes is somewhat better. Model ion exchange systems containing these sites at large or moderate separation correspond to alkali aluminosilicate and silicate glass systems. In these glasses the site separation of the pairs of sites considered in the calculations corresponds to the average distance between negative sites in the glass which depends on the mole percent of alkali oxides. One such glass for which the exchange constants have been determined has the composition (in mole percent) Na_2O - 11; Al_2O_3 - 18; SiO_2 - 71. This glass has a K_{NaCa} of less than 0.0002 (Eisenman and others, 1957). The separation of sites in this glass is approximately 5.8 Å[*].

---

[*] Calculated on an assumed glass density of 2.5 grams cc^{-1} which leads to a molal volume of 26.14 cc $mole^{-1}$ and to a Na^+ density of 5.07×10^{21} atoms cc^{-1}.

The predicted K_{NaCa} (figure 5) for this separation is extremely small (K_{NaCa}(calc) 10^{-65}). However, 40 mole percent of Na_2O in a sodium aluminosilicate glass would lead to a predicted K_{NaCa} of 0.05 (ΔU_r in figure 5 = 1.8 Kcal mole^{-1}).

Some of the natural glasses studied have K_{NaCa} values up to 0.05 and have less than ten mole percent total alkalies. These glasses also contain divalent oxides and it seems probable that exchange is taking place at the paired sites originally occupied by these divalent ions. In these and other aluminosilicate glasses containing divalent cations, the site separation of the paired sites is independent of the total number of sites in the glass and depends chiefly on the radius of the divalent ion in the original glass composition.

Figure 7 has been calculated for paired sites groups about Ca^{++} ion. The predicted sequence of selectivity for values of the anionic radii greater than 1.25 Å*/ is (decreasing preference) $K^+ > Na^+ > Li^+ > Ca^{++} > Mg^{++}$. This is the sequence found for all the glasses tested and is that observed by Jenny (1936) for some clay minerals.

Although the other calculated energy changes are reasonable, that of the Ca-Mg exchange is much too large compared with the experimental value. This suggests that MgO in the glass forms sites with a greater preference for Mg^{++} ions. This is shown in figure 8, where the K_{MgCa} observed is plotted against the mole ratio of CaO-MgO.

Eisenman (1961b) observed that the Na-K selectivity was related

---

*/ A reasonable value since the radius of an oxygen ion is about 1.4 Å.

to the M^{+}-Al^{+3} ratio, however, a plot for the natural glasses studied does not show a correlation and this should make us cautious about attempting to predict the ion exchange behavior of complex glass systems from that of simpler ones.

On the basis of the same reasoning the Na-Ca selectivity of a glass should be related to its content of monovalent, divalent and trivalent oxides. Figure 10 shows, however, that except for glasses with the larger constants tending to have a lower alumina content, no relation is evident.

On the assumption that the effective anionic radius determines the selectivity between like charged cations (Eisenman, 1961a) there should be a definite correlation between K_{MgCa} and K_{NaK}, K_{NaH} and K_{KH}. These quantities are plotted in figures 11, 12 and 13. The general positive correlation between K_{MgCa} and K_{NaH} and K_{KH} indicates that H^{+} enters the glass as the hydronium ion H_3O^{+} since it behaves as a large cation. This is supported by the finding that hygroscopicity and pH selectivity are directly related (Hubbard, 1946).

The results shown in figures 8, 12 and 13 suggest a relation between preference for H^{+} and increasing CaO-MgO ratio. Figure 14 shows this more clearly and suggests that calcium rich glasses should be less stable in waters of low pH. The equilibrium composition of water in contact with large quantities of glass and of glass in contact with large quantities of water can be calculated from the compositions of the glass and the water and the constants K and B as was indicated earlier (Truesdell, 1962).

Bibliography

Eisenman, G., Rudin, D. O. and Casby, J. U., 1957, Glass Electrode for Measuring Sodium Ion: Science 126, 831.

Eisenman, G., 1961a, On the Elementary Atomic Origin of Equilibrium Ionic Specificity: Symposium on Membrane Transport and Metabolism, Czech. Acad. Sciences, Prague.

Eisenman, G., 1961b, Cation Selective Glass Electrodes and their Mode of Operation: The Biophysical Journal (in Press).

Evans, R. C., 1952, An Introduction to Crystal Chemistry, Publishers to the University, Cambridge, p. 171.

Garrels, R. M., Sato, M., Thompson, M. E. and Truesdell, A. H., 1962, Glass Electrodes Sensitive to Divalent Cations: Science 135, 1045.

Green, J., 1959, Geochemical Table of the Elements: Geol. Soc. Amer. Bull., 70, 1127.

Hubbard, D., 1946, Journal of Research: Natl. Bur. Standards, 37, 223.

Jenny, H., 1936, Simple Kinetic Theory of Ion Exchange I: J. Phys. Chem., 40, 501.

Truesdell, A. H., 1962, Study of Natural Glasses through their Behavior as Membrane Electrodes: Nature (in Press).

Waddington, T. C., 1959, Lattice Energies and their Significance in Inorganic Chemistry, in H. J. Emeleus and A. G. Sharp, eds., Advances in Inorganic Chemistry and Radiochemistry, v. 1, Academic Press, New York.

Rossini, F. D., Wagman, D. D., Evans, W. H., Levine, S., and Jaffe, I., 1952, Selected Values of Chemical Thermodynamic Properties: Natl. Bur. Standards Circ. 500.

Table 1a. Analyses of glasses studied in weight percent*

	SiO_2	Al_2O_3	Fe_2O_3	FeO	MgO	CaO	Na_2O	K_2O	H_2O	Total
NG8	97.58	1.54	0.0	0.23	0.0	0.38	0.34	0.0	0.10	100.17
SG1	86.4	8.2	2.10[a]	n.d.	1.3	0.00	0.21	0.95	n.d.	99.16
B20	78.37	12.21	0.05	3.33	0.67	0.78	1.84	2.43	0.0	99.68
NG7	74.7	11.7	1.25[a]	n.d.	0.1	0.62	3.6	5.10	n.d.	97.18
NG5	75.8	12.1	1.85[a]	n.d.	0.6	0.70	3.4	5.15	n.d.	99.86
NG2	75.4	13.9	1.20[a]	n.d.	0.4	0.00	4.1	4.57	n.d.	99.74
B76	74.94	14.81	0.13	4.68	0.43	0.66	1.50	1.84	0.0	98.99
ST2	76.05	13.94	0.21	2.06	1.68	0.96	1.46	2.29	0.0	98.65
B90	71.89	17.56	0.27	5.26	0.78	0.45	1.28	1.60	0.0	99.09
NG6	71.8	13.5	4.75[a]	n.d.	2.5	2.80	1.4	2.45	n.d.	100.14
SG2	70.3	21.5	1.05[a]	n.d.	0.2	0.83	3.5	3.50	n.d.	100.88
SG3	58.0	21.3	6.10[a]	n.d.	2.4	5.88	4.6	1.20	n.d.	99.48
SG4	46.5	35.2	4.65[a]	n.d.	0.9	2.50	7.4	5.02	n.d.	102.17

*In order of decreasing mole % SiO_2.

a/ (For this and other footnotes see following page).

Table 1a (Continued)

[a] Total iron is expressed as Fe_2O_3.

n.d. not determined.

NG8 Libyan Desert glass, Africa; analysis from P. A. Clayton, and L. J. Spencer, Mineral Mag., 23, 501, 1934.

SG1 Synthetic Darwin glass; analysis by H. J. Rose, Jr., F. J. Flanagan, and L. Shapiro.

B20 Bediasite, (tektite), Lee County, Texas; analysis by M. K. Carron, and F. Cuttitta.

NG7 Obsidian, Obsidian Cliffs, Yellowstone, Wyoming; analysis by H. J. Rose, Jr., F. J. Flanagan, and L. Shapiro. Also contains MnO, 0.03% and TiO_2, 0.08%.

NG5 Walcott welded tuff, American Falls Quad, Idaho; analysis by H. J. Rose, Jr., F. J. Flanagan, and L. Shapiro. Also contains MnO, 0.05% and TiO_2, 0.21%.

NG2 Puerto de Abrigo Obsidian, Jamez Caldera, New Mexico; analysis by H. J. Rose, Jr., F. J. Flanagan, and L. Shapiro. Also contains MnO, 0.07% and TiO_2, 0.10%.

B76 Bediasite, Lee County, Texas; analysis by M. K. Carron, and F. Cuttitta.

ST2 Synthetic tektite; analysis by M. K. Carron, and F. Cuttitta.

B90 Bediasite, Lee County, Texas; analysis by M. K. Carron, and F. Cuttitta.

NG6 Tektite, Marulas, P. I.; analysis by H. J. Rose, Jr., F. J. Flanagan, and L. Shapiro. Also contains MnO, 0.13% and TiO_2, 0.81%.

SG2 Synthetic tektite (Peru); analysis by H. J. Rose, Jr., F. J. Flanagan, and L. Shapiro.

SG3 Synthetic Fulgerite (Armenia); analysis by H. J. Rose, Jr., F. J. Flanagan, and L. Shapiro.

SG4 Synthetic obsidian (Mt. Vesuvius); analysis by H. J. Rose, Jr., F. J. Flanagan, and L. Shapiro. This glass has 15% more Al_2O_3 and 7% less SiO_2 than was intended.

Table 1b. Analyses of natural glasses in mole percent (water free)

	SiO_2	Al_2O_3	Fe_2O_3*	FeO*	MgO	CaO	Na_2O	K_2O
NG8	98.16	0.91	0.0	0.19	0.0	0.40	0.33	0.0
SG1	91.17	5.09	0.83	—	2.06	0.0	0.21	0.64
B20	84.19	7.71	0.02	2.52	1.08	0.90	1.91	1.67
NG7	83.37	7.68	0.52	—	0.17	0.74	3.89	3.63
NG5	82.54	7.75	0.76	—	0.98	0.82	3.58	3.58
NG2	82.40	8.93	0.49	—	0.66	0.0	4.34	3.19
B76	81.84	9.51	0.05	4.26	0.70	0.77	1.59	1.28
ST2	81.34	8.76	0.08	1.84	2.69	1.10	1.51	1.56
B90	79.34	11.39	0.11	4.84	1.29	0.53	1.37	1.13
NG6	78.74	8.70	1.95	—	4.11	3.29	1.49	1.72
SG2	77.99	14.02	0.44	—	0.33	0.99	3.76	2.48
SG3	65.96	14.24	2.60	—	4.09	7.17	5.06	0.87
SG4	55.80	24.83	2.09	—	1.62	3.21	8.59	3.84

* see notes for Table 1a.

Table 2a. Exchange constants for some glasses at 25°C, 1 atm.

	K_{NaH}	K_{KH}	K_{NaK}	K_{NaCa}	K_{KCa}	K_{NaMg}	K_{MgCa}
NG8	13	5.7	2.2	0.010	0.0021	0.0053	1.6
SG1	47	5.9	3.3	0.010	0.00081	0.0015	2.3
B20	19	4.6	3.6	0.0081	0.00069	0.0014	2.7
NG7	60	27	2.8	0.0056	0.00076	0.0015	3.1
NG5	3.5	1.4	2.4	0.050	0.020	n.d.	1.0
NG2	3.2	1.3	2.5	0.042	0.014	n.d.	1.0
B76	21	4.6	3.4	0.0078	0.0012	0.0023	2.1
ST2	34	7.2	2.7	0.0067	0.00091	0.01	1.1
B90	12	4.9	2.2	0.0069	0.0014	0.0059	1.1
NG6	3.0	1.5	2.0	0.047	0.023	n.d.	1.6
SG2	54	12	2.6	0.0040	0.00068	0.0015	2.7
SG3	35	13	3.0	0.010	0.0022	0.0062	1.6
SG4	19	7.9	2.4	0.0087	0.0019	0.0045	1.6

n.d./ (For this and other footnotes see following page)

Table 2a (Continued)

n.d., not determined.

Constants for NG5, NG2 and NG6 which have been published previously are repeated here to facilitate comparisons.

K values obtained were from the electrode equations:

$$E = E^\circ + \frac{2.303RT}{\mathcal{F}} \log\left(\frac{[A^+]}{\lambda_{AX}} + K_{AB}\frac{[B^+]}{\lambda_{BX}}\right),$$

$$E = E^\circ + \frac{2.303RT}{2\mathcal{F}} \log\left(\frac{[A^+]^2}{\lambda_{A_2X_2}} + K_{AB}\frac{[B^{++}]}{\lambda_{BX_2}}\right),$$

or $$E = E^\circ + \frac{2.303RT}{2\mathcal{F}} \log\left(\frac{[A^{++}]}{\lambda_{AX_2}} + K_{AB}\frac{[B^{++}]}{\lambda_{BX_2}}\right),$$

where $$\lambda_{AX} = \exp\left(\frac{B_{AB}}{RT}(1 - N_{AX})^2\right)$$

Table 2b. B_{AB} values in Kcal mole^{-1} for some glasses at 25°C and 1 atm.

	B_{NaH}	B_{KH}	B_{NaK}	B_{NaCa}	B_{KCa}	B_{NaMg}	B_{MgCa}
NG8	0.0	+0.3	+0.3	+0.1	0.0	-0.1	+0.2
SG1	+0.2	-1.2	+0.2	+0.3	+0.3	+0.3	-0.2
B20	+0.3	-0.3	+0.2	+0.3	+0.5	+0.4	n.d.
NG7	-0.5	+0.1	+0.1	+0.4	0.0	+0.2	+0.3
NG5	-0.5	+0.4	n.d.	n.d.	-0.5	n.d.	0.0
NG2	-0.2	-0.6	-0.2	-0.2	+0.2	n.d.	n.d.
B76	+0.3	-0.6	+0.1	+0.1	0.0	0.0	+0.3
ST2	+0.3	n.d.	+0.3	n.d.	+0.3	n.d.	n.d.
B90	-0.4	-0.6	n.d.	+0.3	-0.1	+0.3	+0.5
NG6	-0.4	0.0	n.d.	-0.4	-0.5	n.d.	0.0
SG2	+0.4	n.d.	-0.6	+0.3	+0.3	n.d.	+0.3
SG3	+0.5	-1.0	+0.4	+0.2	+0.2	+0.2	+0.4
SG4	-0.9	-1.8	+0.3	+0.3	+0.1	0.0	n.d.

n.d. not determined.

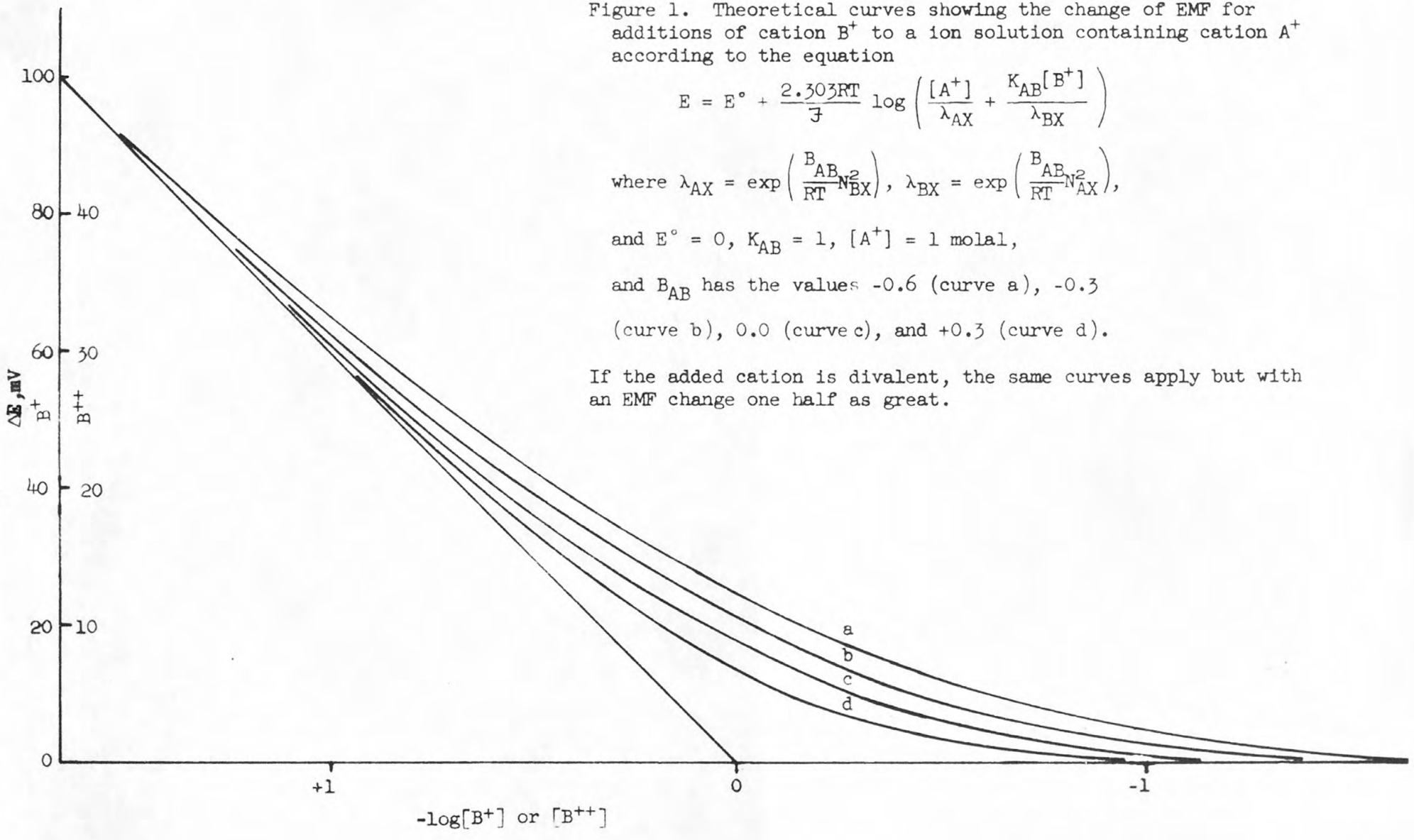

Figure 1. Theoretical curves showing the change of EMF for additions of cation B^+ to a ion solution containing cation A^+ according to the equation

$$E = E^\circ + \frac{2.303RT}{\mathcal{F}} \log \left(\frac{[A^+]}{\lambda_{AX}} + \frac{K_{AB}[B^+]}{\lambda_{BX}} \right)$$

where $\lambda_{AX} = \exp\left(\frac{B_{AB}}{RT} N_{BX}^2 \right)$, $\lambda_{BX} = \exp\left(\frac{B_{AB}}{RT} N_{AX}^2 \right)$,

and $E^\circ = 0$, $K_{AB} = 1$, $[A^+] = 1$ molal,

and B_{AB} has the values -0.6 (curve a), -0.3 (curve b), 0.0 (curve c), and +0.3 (curve d).

If the added cation is divalent, the same curves apply but with an EMF change one half as great.

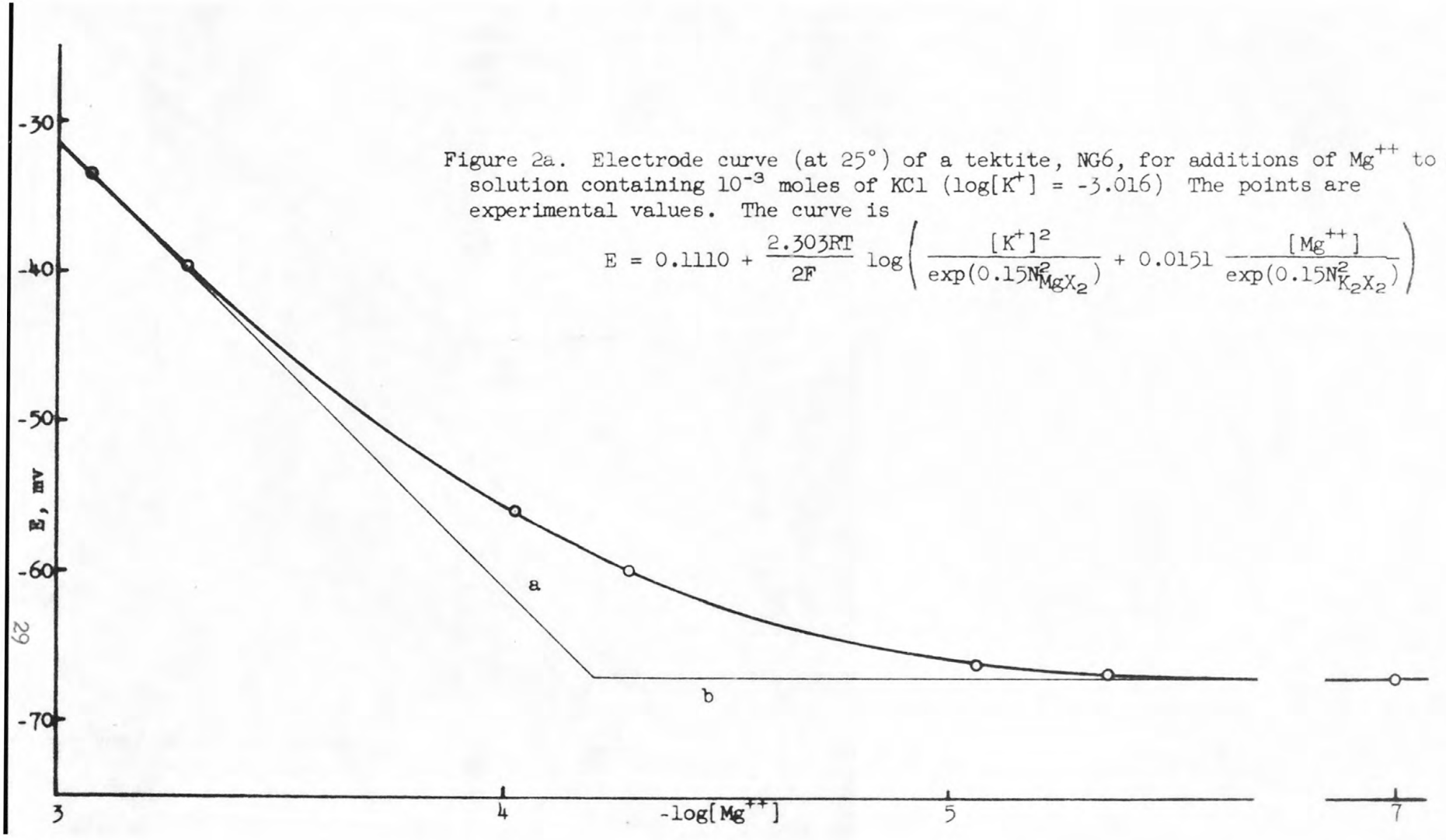

Figure 2a. Electrode curve (at 25°) of a tektite, NG6, for additions of Mg^{++} to a solution containing 10^{-3} moles of KCl ($\log[K^+] = -3.016$) The points are experimental values. The curve is

$$E = 0.1110 + \frac{2.303RT}{2F} \log\left(\frac{[K^+]^2}{\exp(0.15N^2_{MgX_2})} + 0.0151 \frac{[Mg^{++}]}{\exp(0.15N^2_{K_2X_2})} \right)$$

Figure 2b. Electrode curve of a tektite, NG6, for additions of Ca^{++} to a solution containing 10^{-3} mole of KCl ($\log[K^+] = -3.016$) The points are experimental values. The curve is

$$E = 0.1110 + \frac{2.303RT}{2F} \log\left(\frac{[K^+]^2}{\exp(-0.9N^2_{CaX_2})} + 0.0234 \frac{[Ca^{++}]}{\exp(-0.9N^2_{K_2X_2})}\right)$$

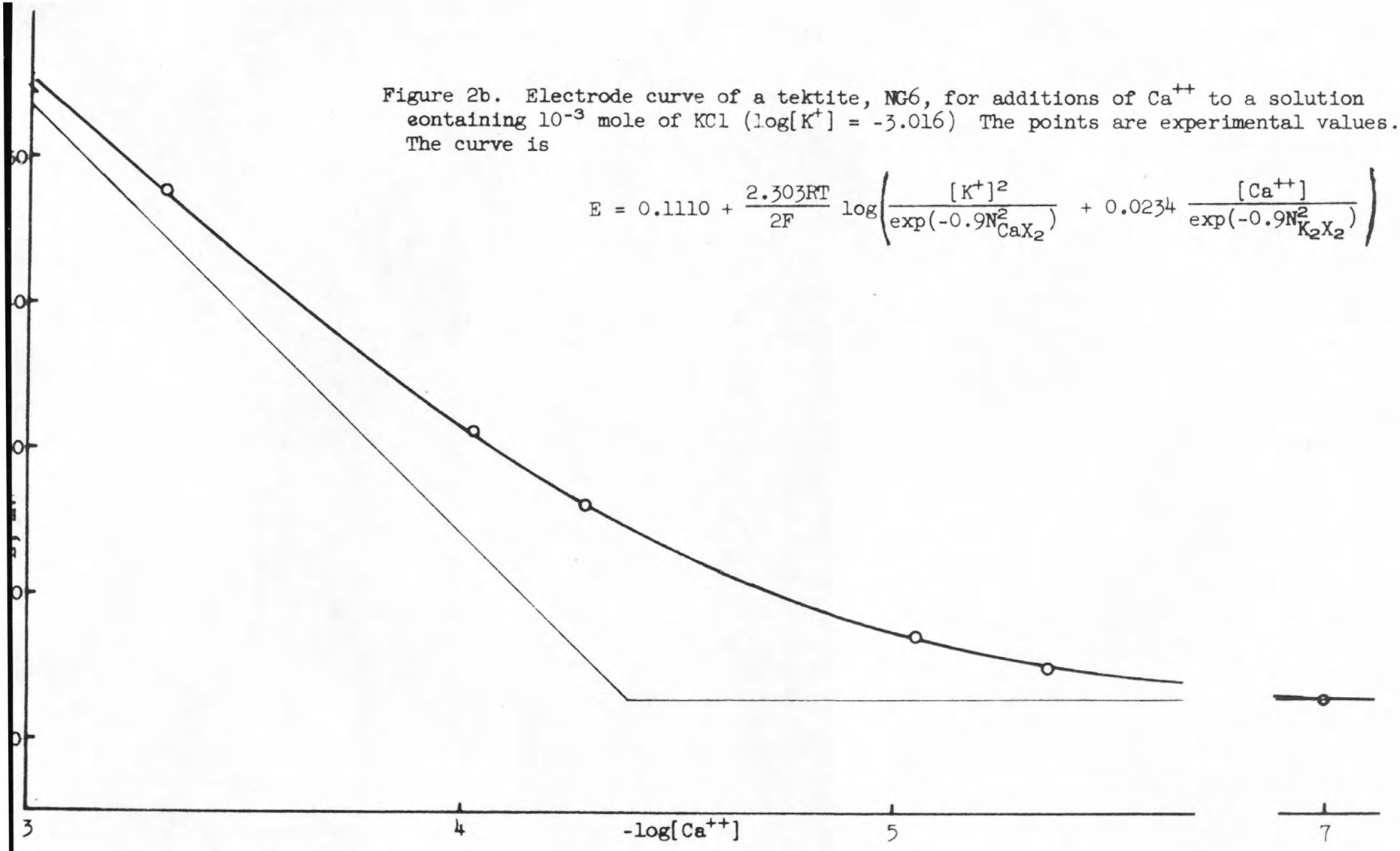

Figure 3. Configurations of cations and anionic sites of model ion exchange systems

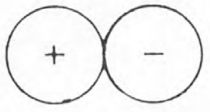

a. monovalent cations and single monovalent sites

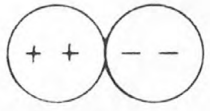

b. divalent cations and divalent sites

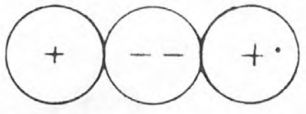

c. monovalent cations and divalent sites

d. monovalent cations and paired monovalent sites with site separation x (position of lowest energy)

e. divalent cations and paired monovalent sites

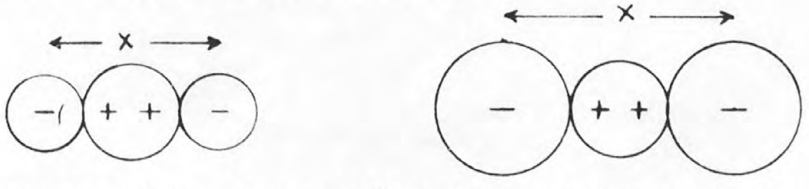

f. paired monovalent sites at the minimum separation about a divalent cation (as r^- increases, x increases)

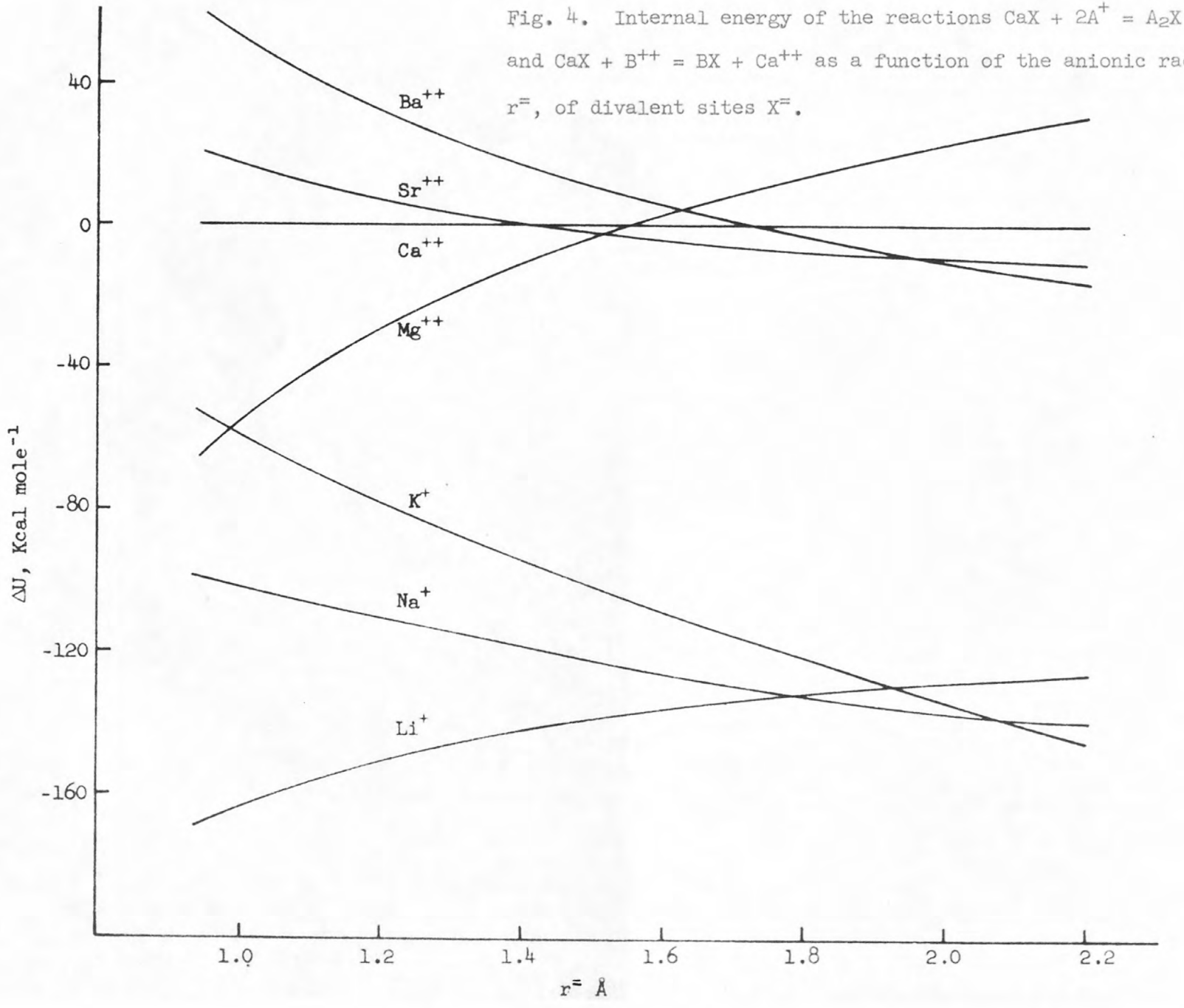

Fig. 4. Internal energy of the reactions $CaX + 2A^{+} = A_2X + Ca^{++}$ and $CaX + B^{++} = BX + Ca^{++}$ as a function of the anionic radius, $r^{=}$, of divalent sites $X^{=}$.

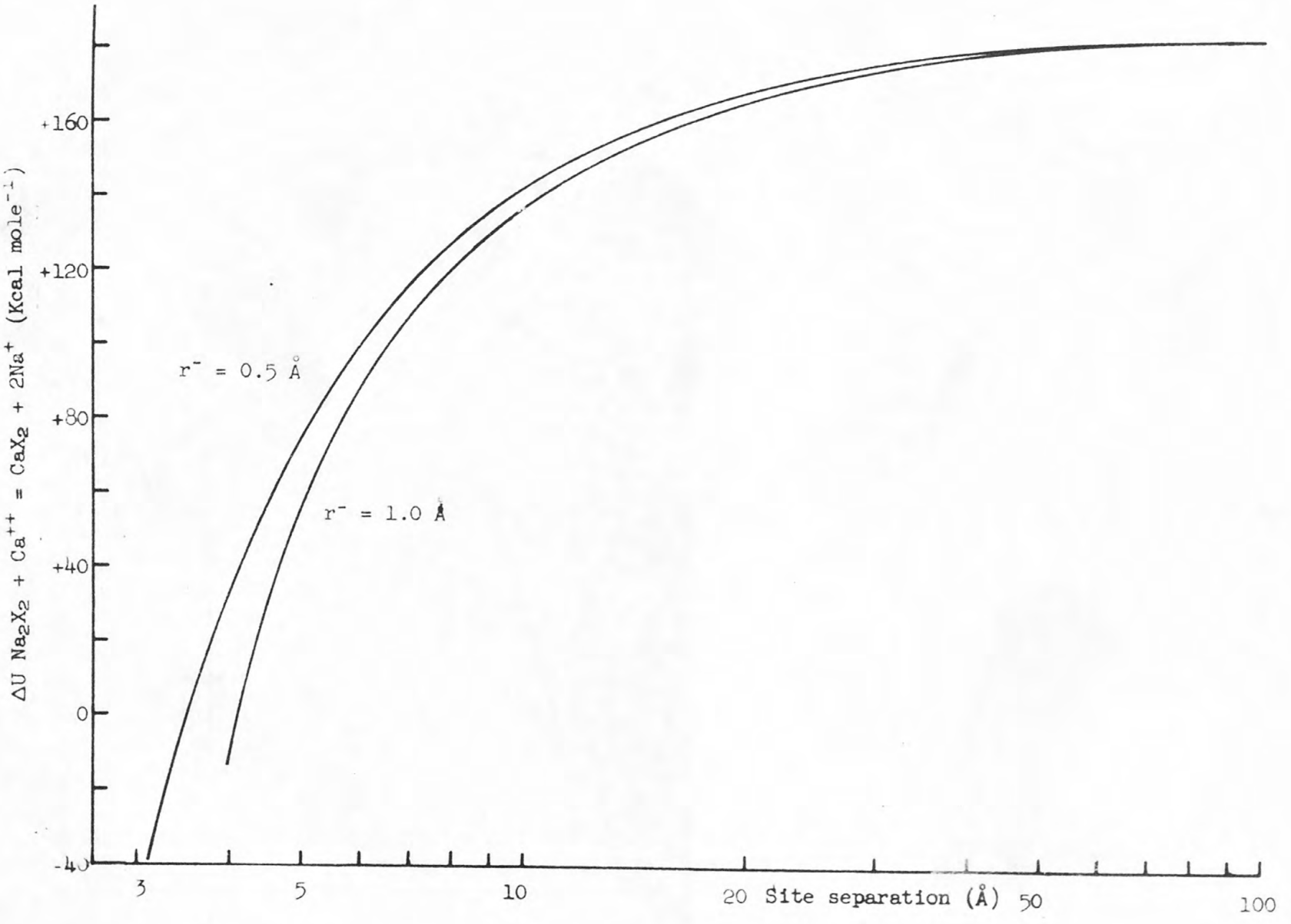

Figure 5. Internal energy of the exchange reaction $Na_2X_2 + Ca^{++} = CaX_2 + 2Na^+$ for paired monovalent sites of $r^- = 0.5$ and 1.0 Å as a function of site separation.

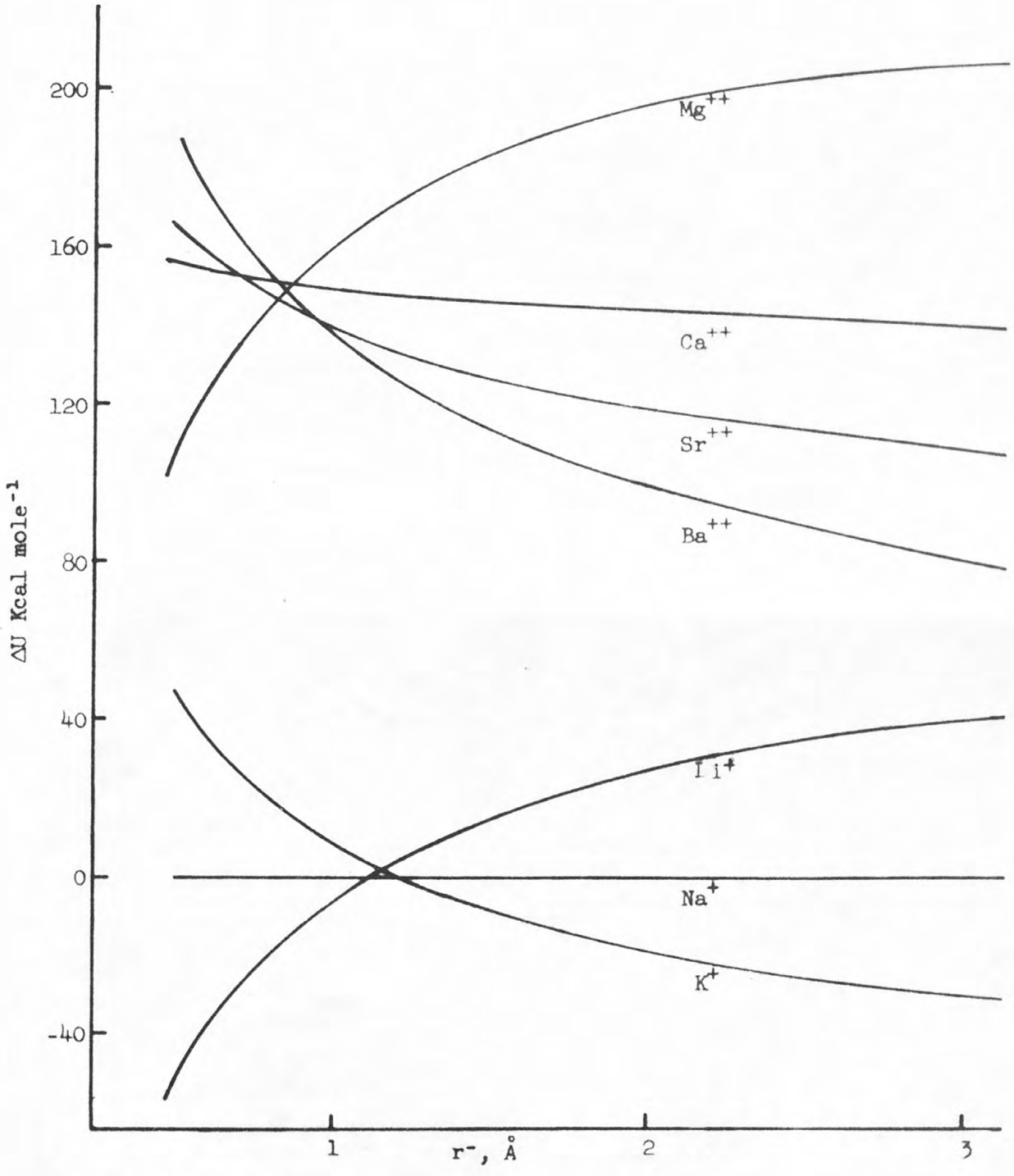

Figure 6a Internal energy of the exchange reactions $Na_2X_2 + 2A^+ = A_2X_2 + 2Na^+$ and $Na_2X_2 + B^{++} = BX_2 + 2Na^+$ as a function of anionic radius r^- of paired monovalent sites at a site separation of 12 Å.

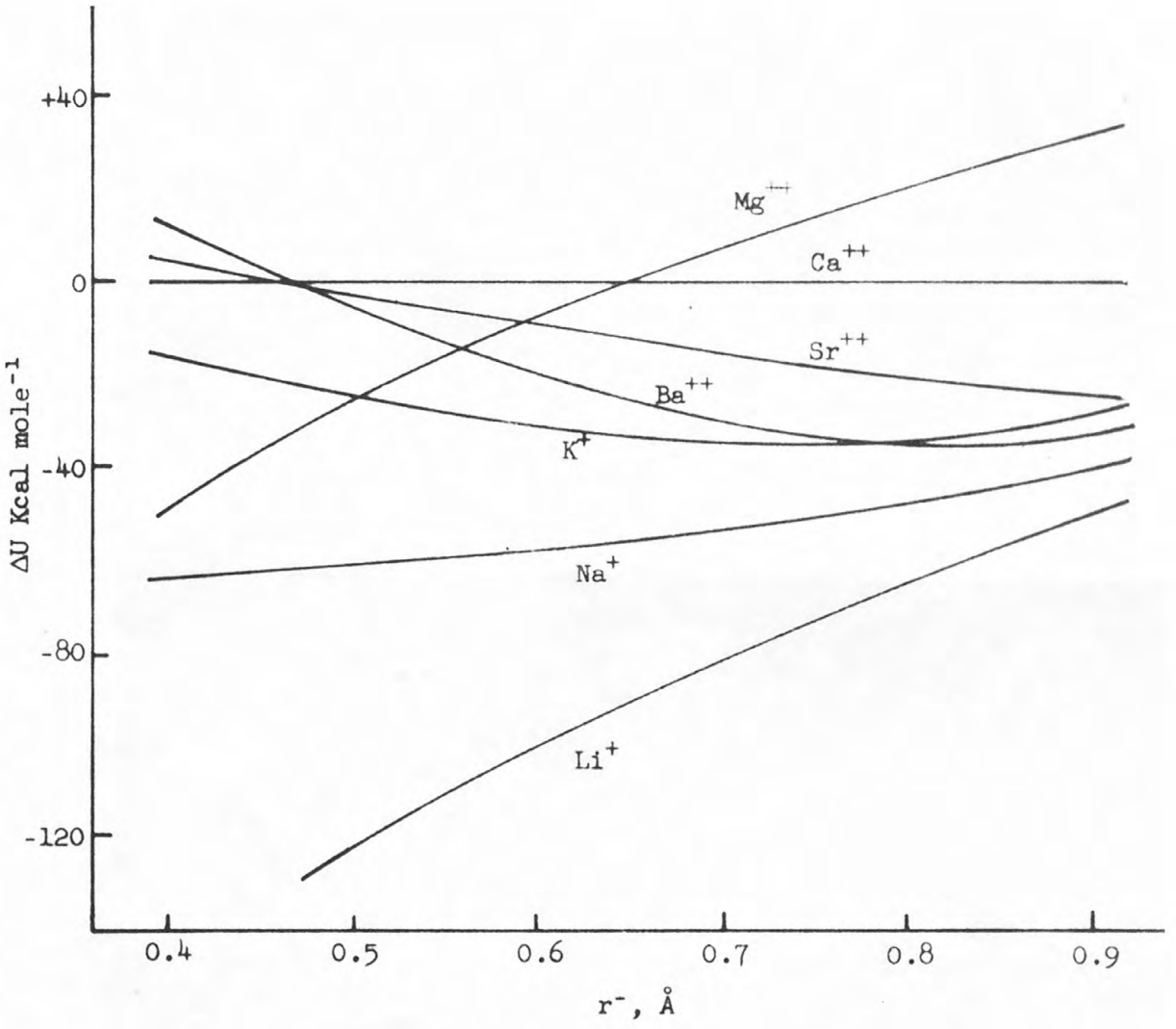

Figure 6. Internal energy of the exchange reactions $CaX_2 + 2A^+ = A_2X_2 + Ca^{++}$ and $CaX_2 + B^{++} = BX_2 + Ca^{++}$ as a function of anionic radius, r^-, of paired monovalent sites at a separation of 4.5 Å.

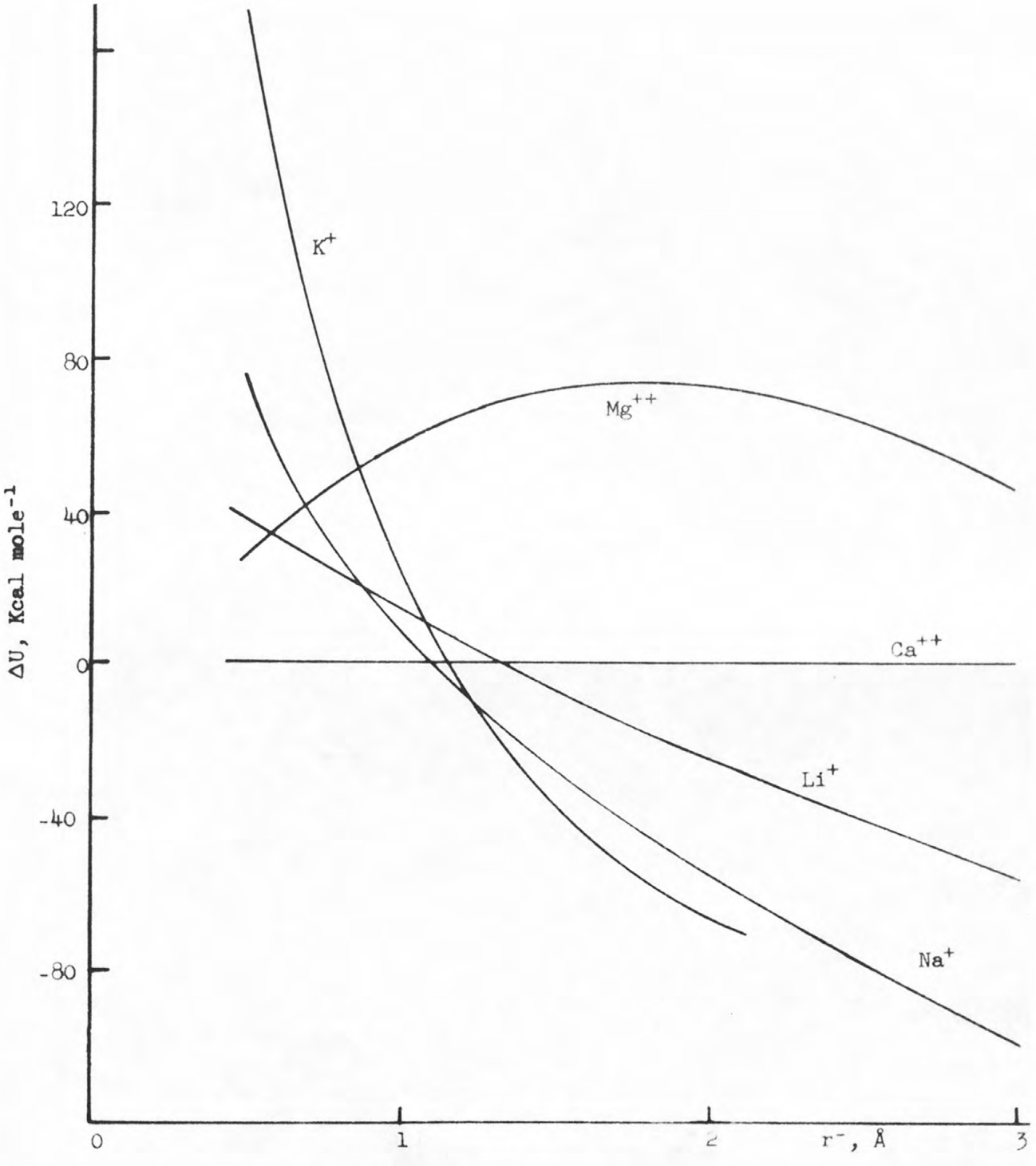

Figure 7. Internal energy of the exchange reactions $CaX_2 + 2A^+ = A_2X_2 + Ca^{++}$ and $CaX_2 + B^{++} = BX_2 + Ca^{++}$ as a function of anionic radius, r^- of paired monovalent sites at the distance of closest approach to a Ca^{++} ion.

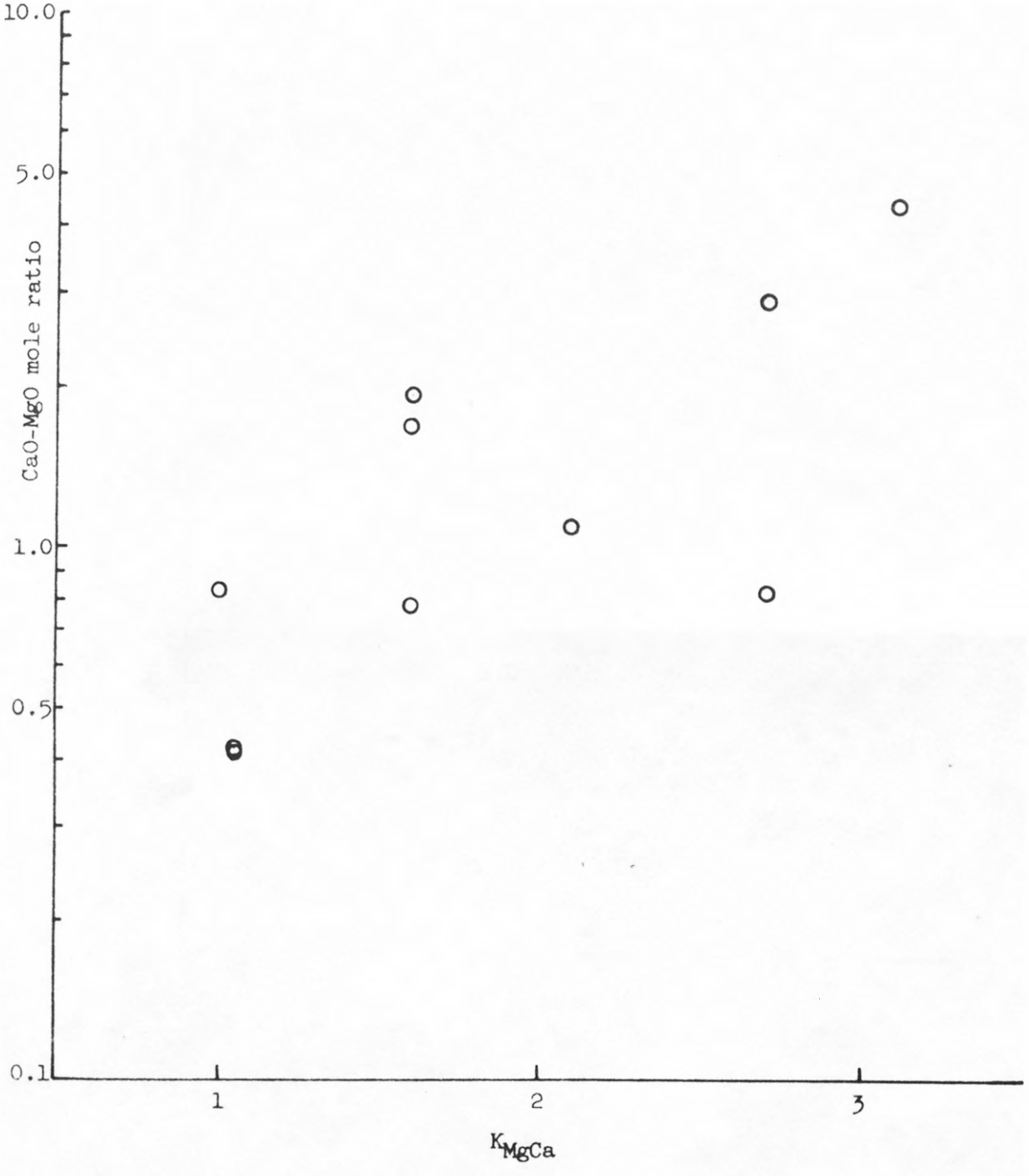

Figure 8. Plot of K_{MgCa} against CaO-MgO mole ratio for some natural glasses.

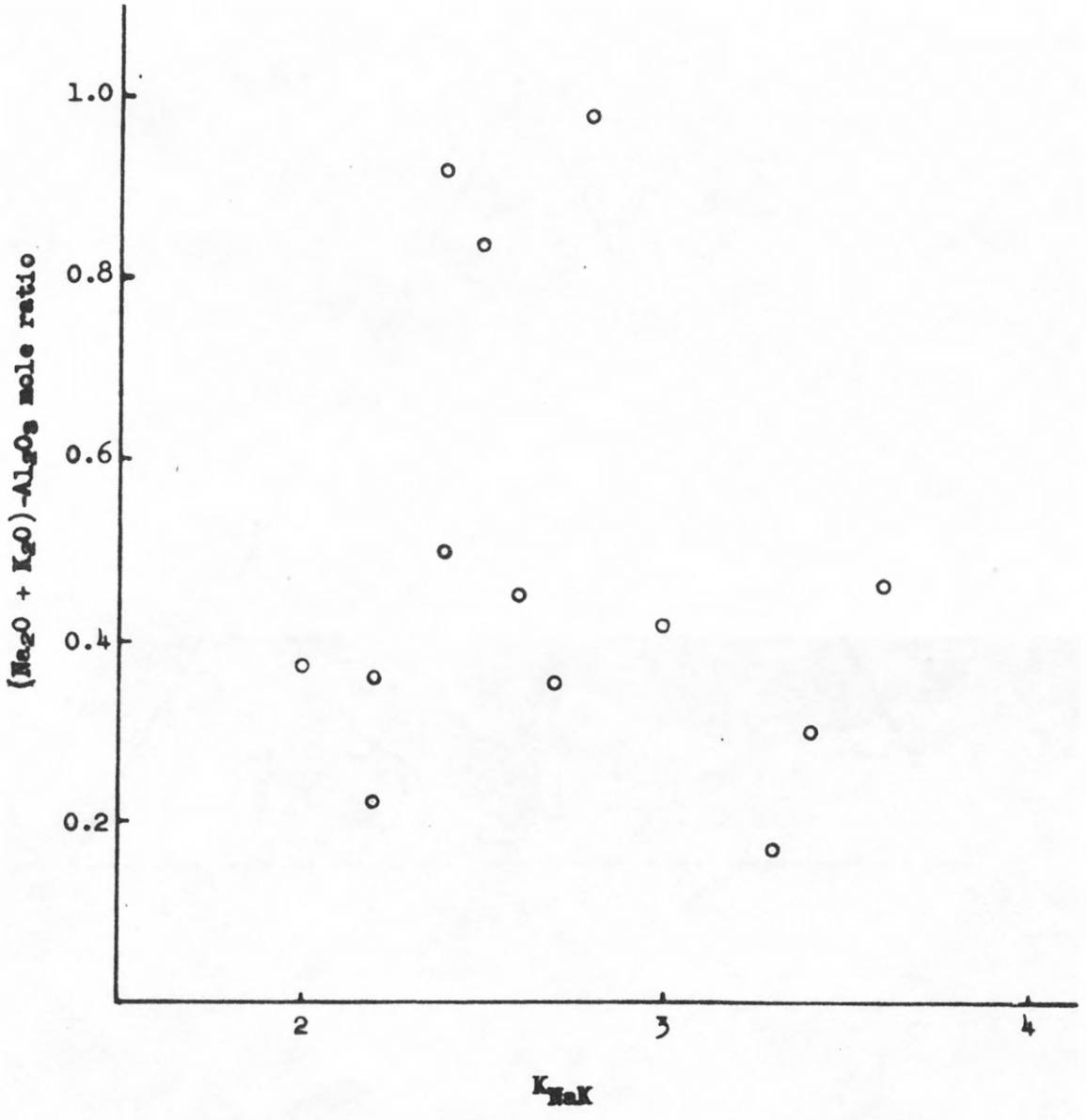

Figure 9. Plot of K_{NaK} against $(Na_2O + K_2O)$-Al_2O_3 mole ratio.

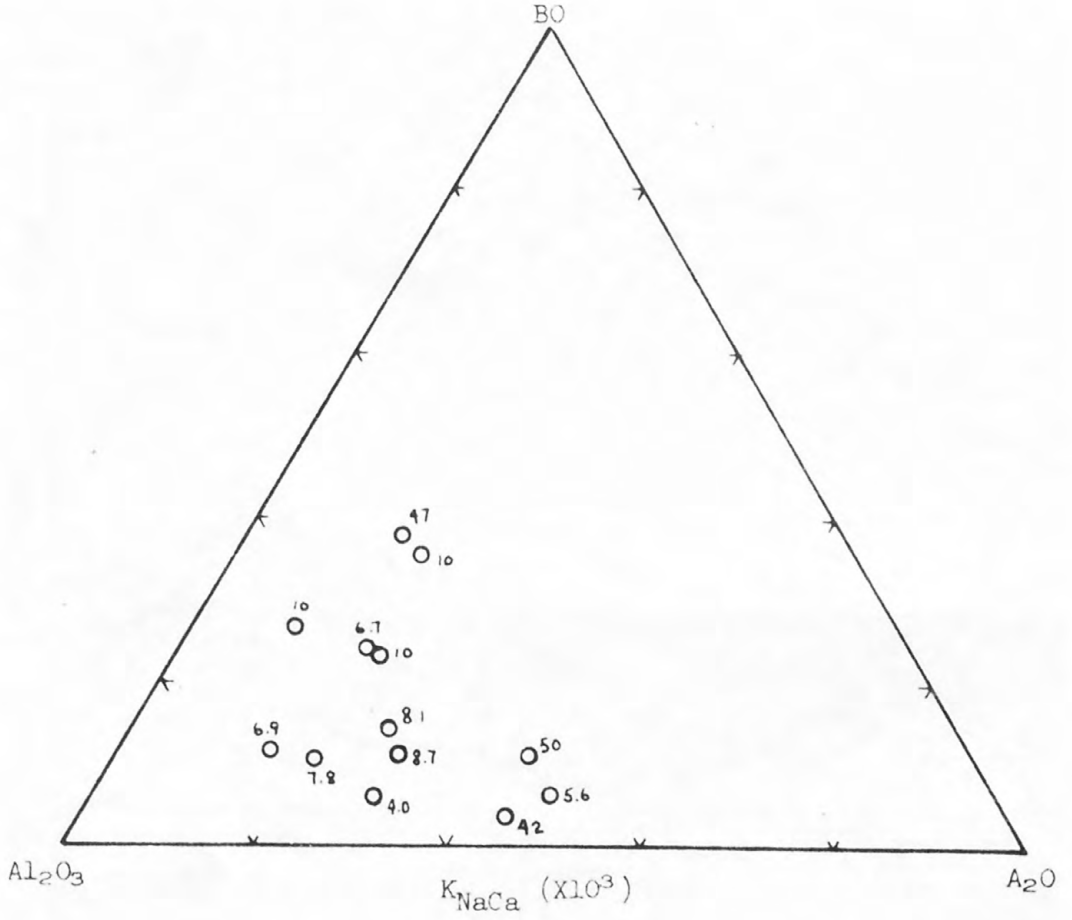

Figure 10. Plot of K_{NaCa} ($X10^3$) values against content of monovalent, divalent (excluding FeO) and trivalent (excluding Fe_2O_3) oxides.

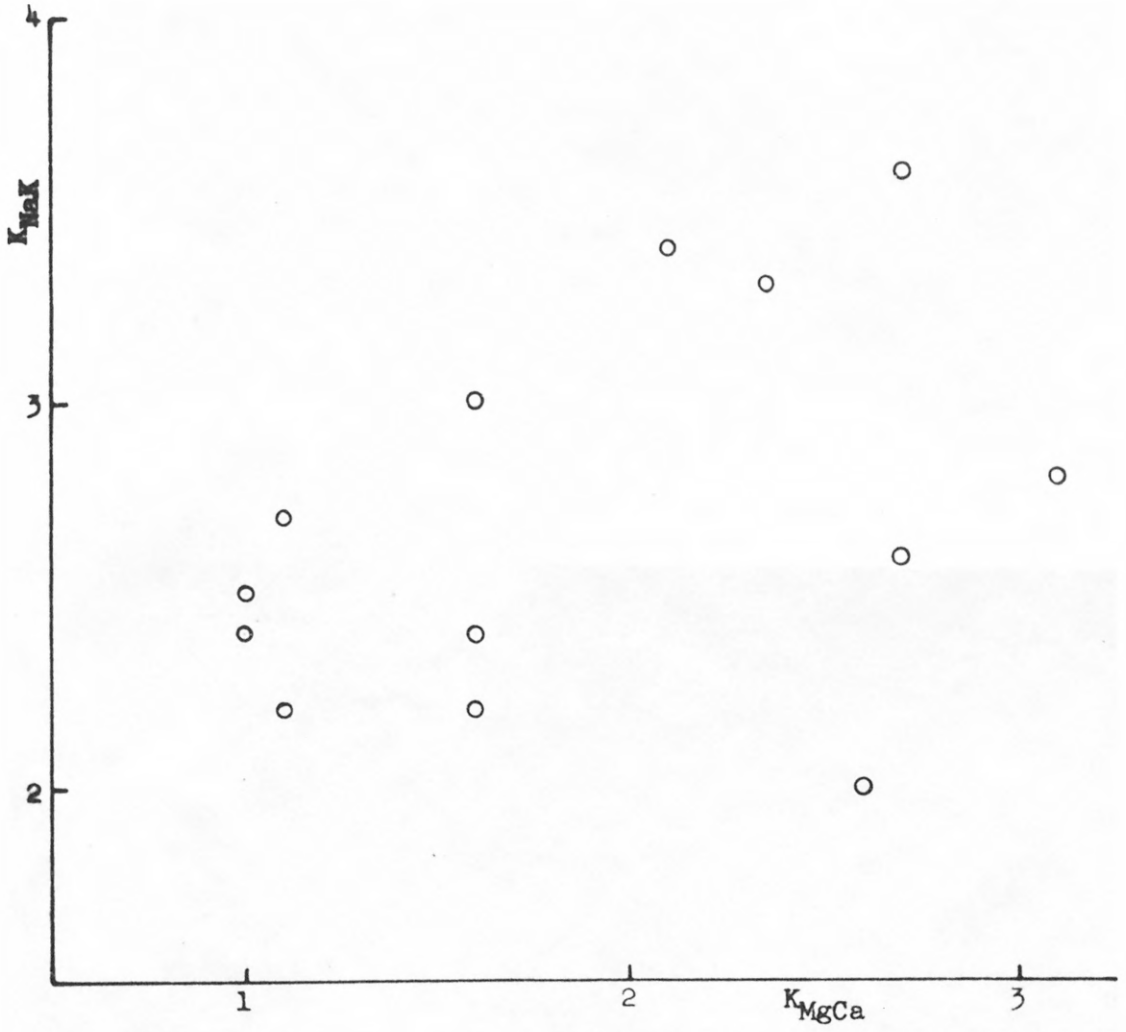

Figure 11. Plot of K_{MgCa} against K_{NaK} for some natural glasses.

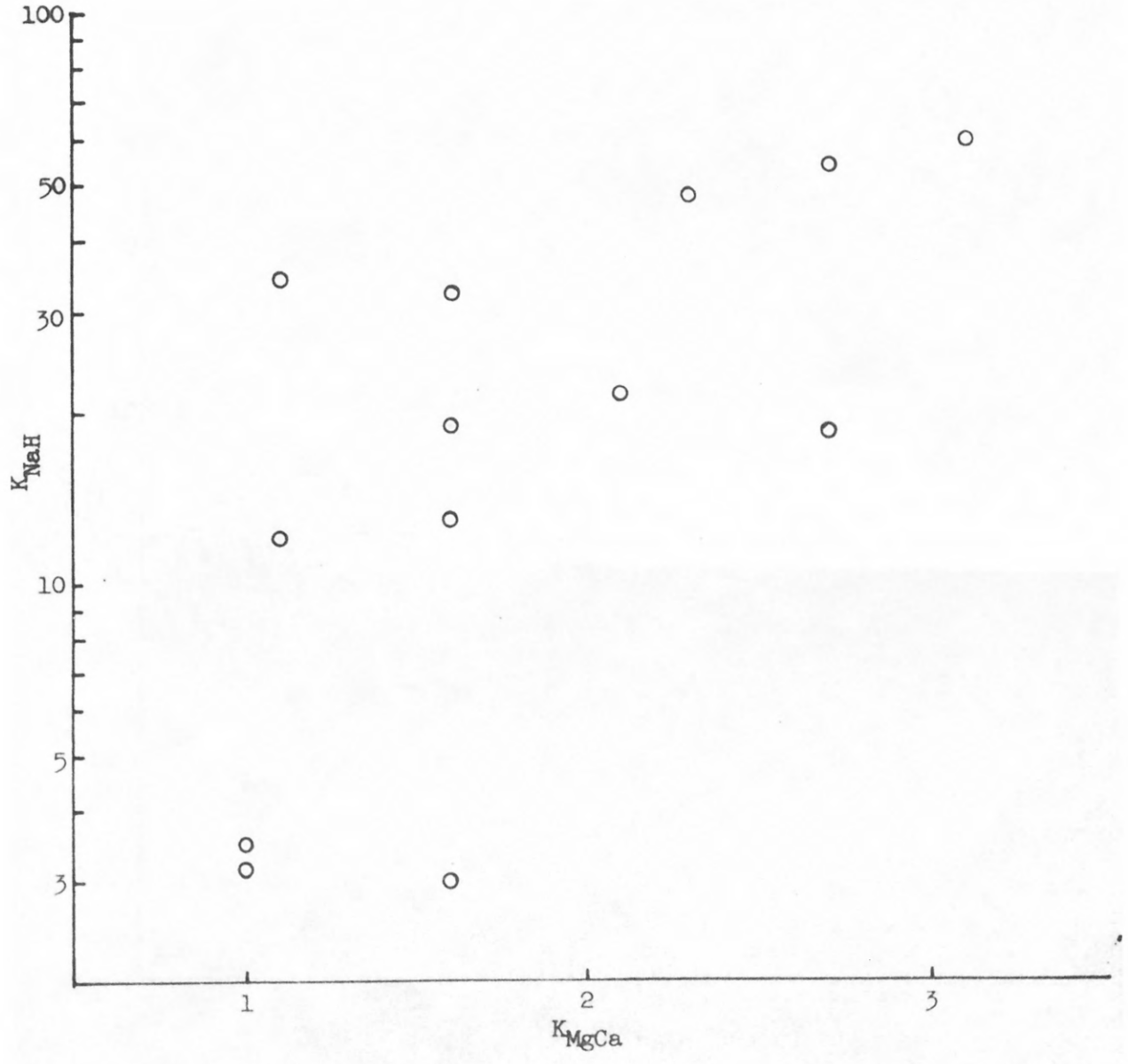

Figure 12. Plot of K_{MgCa} against K_{NaH} for some natural glasses.

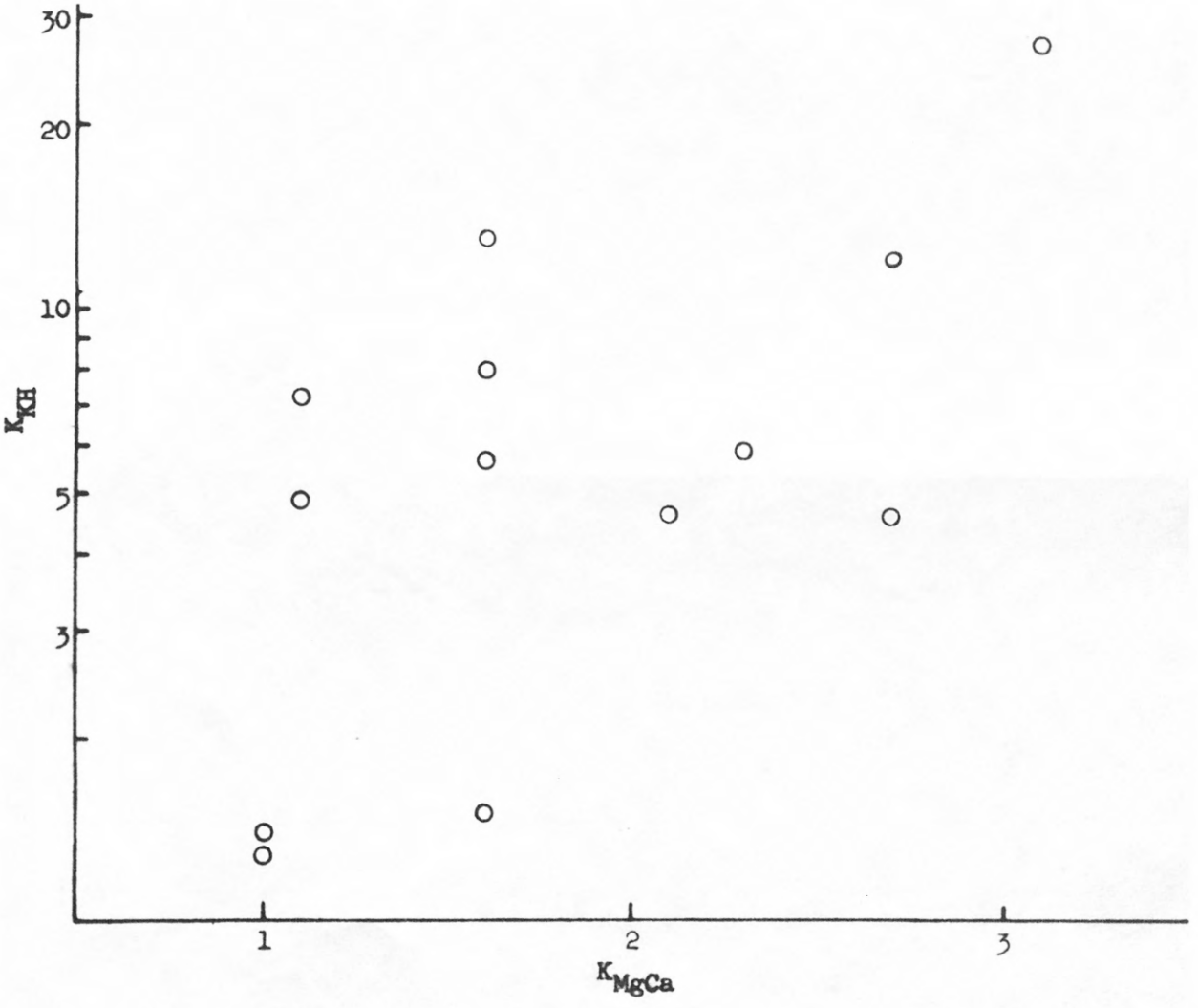

Figure 13. Plot of K_{MgCa} against K_{KH} for some natural glasses

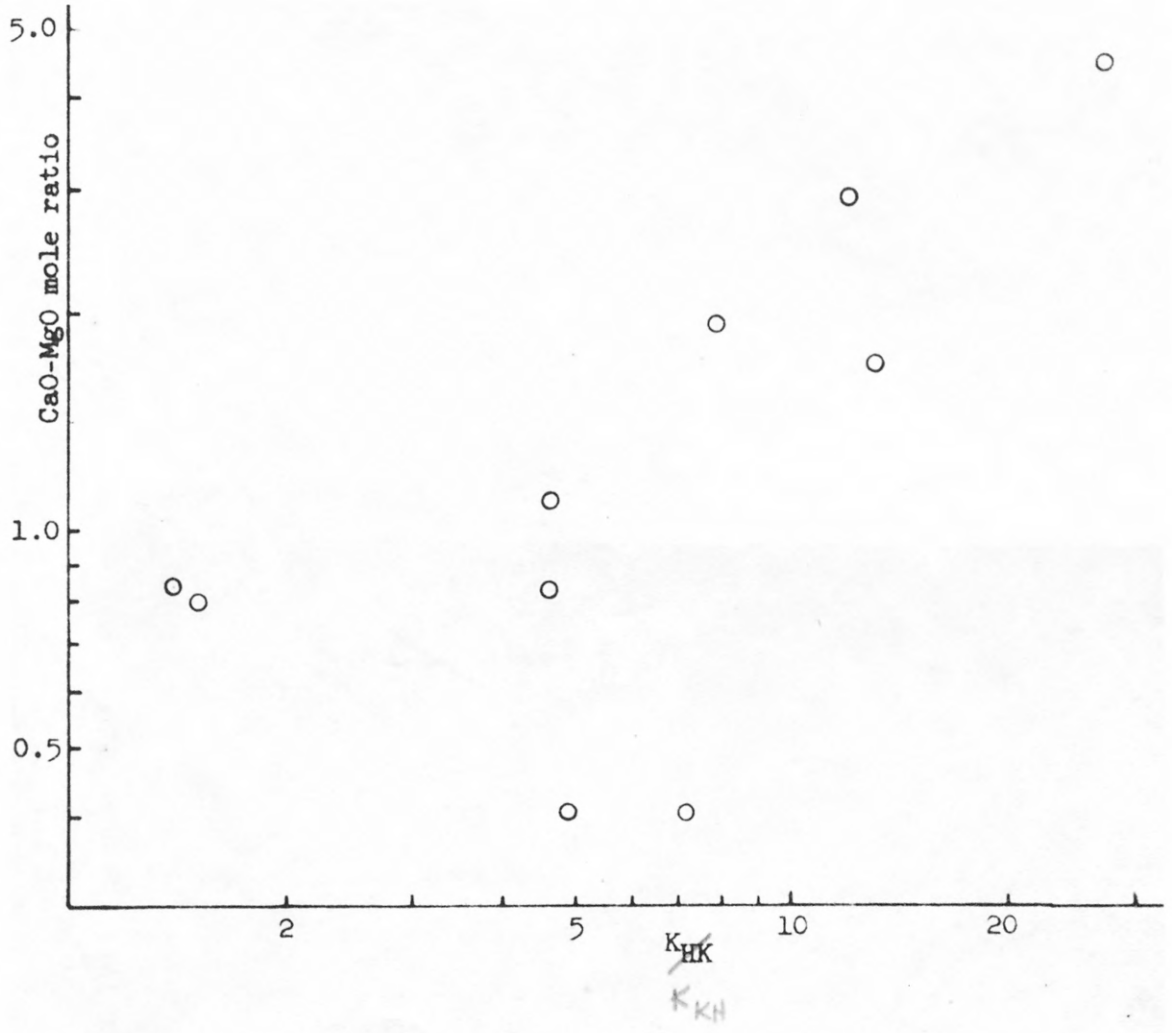

Figure 14. Plot of K_{HK} against CaO-MgO ratio for some natural glasses